PLEASE DO NOT REMOVE THIS PAGE

Radiative and nonradiative decay rates in chromium-related centers in nanodiamonds

S. Castelletto[1,2,*] and A. Boretti[3]

[1]*School of Physics, The University of Melbourne, Parkville, VIC 3010, Australia*

[2]*Centre for Micro-Photonics, Swinburne University of Technology, John Street PO Box 218, Hawthorn, VIC 3122, Australia*

[3]*Department of Mechanical and Aerospace Engineering, Missouri University of Science and Technology, 280 Toomey Hall, Rolla, Missouri 65409, USA*

*Corresponding author: sacas@unimelb.edu.au

We address for the first time the measurement of nonradiative decay rates in Cr-related centers in nanodiamonds. Compared to our previous quantum efficiency measurement of Cr centers created in bulk diamond, separate measurements of radiative and nonradiative decay rates in grown nanodiamonds prove more challenging due to size dependence effects. We demonstrate in this Letter that, using defocused dipole imaging and collection efficiency calculation via finite-difference time-domain (FDTD), a quantum efficiency up to 0.9 can be inferred to Cr-related centers showing a 2-level system photon statistics.   © 2011 Optical Society of America

OCIS codes: 160.2220, 160.2540, 160.4236, 180.1790.

Color centers in nanodiamonds (NDs) have recently attracted much attention due to their application as single photon sources in quantum communication [1], as probes for magnetometry [2] and electric field measurements, as ideal emitters for super-resolution imaging [3], mostly due to their photo-stability. In particular, the best-known and most attractive color center, based on a nitrogen atom and a vacancy in the diamond matrix (NV, nitrogen vacancy), is particularly studied for its electron and nuclear spin optical read-out [4], that makes it a viable candidate for quantum computing. However, NV center presents several drawbacks, such as a broadband emission and a dim zero phonon line at low temperature, only about 4% of its entire spectra. Because of its nonlinear dipole in absorption and emission, constituted by two linear and orthogonal incoherent dipoles, its integration in photonics cavity proves cumbersome preventing for now to achieve strong coupling regime at room temperature, thus hampering its full practical exploitation. Other color centers such SiV, NE8, and recently Cr-related centers, present some interesting features such as narrow bandwidth, narrow spectral emission, and short lifetime and in general they are much brighter than NV centers. A comprehensive review on single photon emitters in diamond can be found in [1]. In particular, the recently Cr-related centers in NDs [5] and bulk diamond [6] have been thoroughly studied up to the point of being the most studied center after NV. Cr is the only non-NV center that has been created efficiently in both NDs and bulk diamond. In bulk diamond via dipole imaging it has been possible to measure its dipole emission orientation and directly the quantum efficiency for the first time at the single emitter level [7]. Quantum efficiency measurements at the single quantum level, i.e. the ratio between radiative decay rate and total decay rate, are particularly difficult and relevant in defect centers in NDs in view of their application in establishing single photon standards and in subdiffration microscopy. Many currently used efficient single photon source fluorophores, such as

terrylene single molecules [8] and CdSe quantum dots [9], were directly proved to have a quantum efficiency close to 1, making them very exciting apart from their nonideal photo-stability. NV centers quantum efficiency in bulk diamond has been indirectly inferred 0.7 [3], while Cr in bulk diamond has been measured to have a quantum efficiency of 0.3. This is possibly due to the present method of fabrication, based on heavy ion beam irradiation, which produces excessive damage in the diamond matrix and other N-related impurities that could quench the centers.

In this Letter we address the measurement of radiative and nonradiative decay rates of Cr-related single emitters in NDs. We identify and study several Cr-related centers in chemical vapor deposition (CVD) NDs grown on a sapphire substrate, as reported in [5]. For the identification purpose, we use a homemade confocal microscope to localize single photon emitters (schematic in Fig. 1). Only single photon emissions are considered in this work, i.e. the normalized second-order temporal correlation function $g^{(2)}(\tau) = \langle I(t+\tau)I(t)\rangle / \langle I(t)^2\rangle$ at zero delay time, $g^{(2)}(0) < 0.5$. $g^{(2)}(\tau)$ gives an indication of the number of
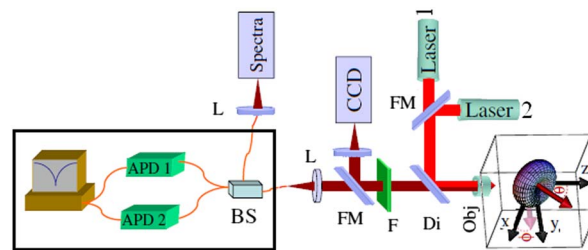

Fig. 1.   (Color online) Schematic of the confocal microscope: Obj $100\times$ 0.95 NA objective, D_i dichroic mirror, F bandpass filters (10 and 40 nm), $APD_{1,2}$ single photon modules, BS beam splitter, FM flipping mirrors, laser 1 and 2 CW and pulsed Ti:sapphs, cooled CCD, spectrum analyzer, photon counting system. The orientation of a generic dipole relative to the optic axis (z) and the sample surface is identified by the polar Θ and azimuthal Φ angles.

emitters in a particular nanocrystal, an "antibunching" dip in $g^{(2)}(\tau)$ indicates sub-Poissonian statistics of the emitted photons. Cr-related centers in NDs are associated with two typical photon statistics, corresponding to either an ideal 2-level system or to a 3-level system, evidenced in the antibunching curve by a photon bunching effect at longer delay times. This is associated to a metastable or dark state, which does not contribute to the measured nonradiative decay rate. In the pulsed regime, we use the laser trigger pulse to measure directly the excited state total lifetime as temporal decay of the photoluminescence. A spectrometer connected to the detection arm allows to measure the emission spectra, reflecting the photon statistics of the single center: narrow bandwidth emitters (1.5 to 4 nm) correspond to 3-level system, while bandwidths of 6–10 nm correspond to a 2-level system. The central peaks of the centers here studied are distributed between 748 nm and 758 nm. The back focal plane of the objective is imaged using a –70 °C cooled CCD to measure the emission dipole orientation via defocused imaging and direct imaging (not shown) methods as described in [7,9]. The transition dipoles orientation angles Θ and Φ can be measured by fitting the cross-section of the direct dipole imaging and the fitted parameters are used to simulate the defocused images shown in Fig. 2. FDTD method was used for the defocused and direct imaging simulations using Lumerical software. Θ and Φ obtained are reported for the some centers in Fig. 2. The orientation of the emission dipole in NDs is randomly distributed. Moreover the excitation of the centers with linearly polarized light and the analysis of the emitted light by a polarizer before the detection, indicate the presence of 1D dipoles both in excitation and emission. The measurement of the dipole orientation is relevant to determine the quantum efficiency of an emitter. The quantum efficiency is defined as $\eta_{qe} = k_{rad}/(k_{rad} + k_{nr})$, where k_{rad} and k_{nr} are the radiative and nonradiative decay rates, respectively. A direct measurement of the total excited state lifetime $\tau_D = (k_{rad} + k_{nr})^{-1}$ is performed for all the emitters. Typical η_{qe} measurements

in nanoscopic single emitters are done by modifying the local density of states in the immediate proximity of the emitter, which induces a calculable modification of only the radiative decay rate. Since the NDs considered here have an average size diameter distribution of about 300 nm and are grown by CVD directly on the substrate, it is not easy to perform such a measurement directly. We therefore measure the count rate for several optical power I and determine the count rate at saturation, R_∞, from the fit $R = R_\infty \times I/(I + I_{sat})$ [Fig. 3(a)]. The count rate at saturation is $R_\infty = \eta_{det} \times \eta_{coll} \times \eta_{qe} \times \tau_D^{-1}$, where $\eta_{det} = 0.44$ is the measured detection efficiency. η_{coll} is the collection efficiency, which is difficult to measure. We can calculate the collection efficiency knowing the polar dipole emission angle Θ. The radiative power $L(\Theta, \Phi, \theta, \phi)$ of a 1D dipole in free space depends on the dipole orientation angles Θ and Φ, as well as on the fluorescence emission angle θ, ϕ. The collection efficiency can be calculated in the case of a dipole embedded in a small ND close to an interface as $\eta_{coll} = \sum_{i=s,p} \int_0^{\arcsin(NA)/n} d\theta \times \sin\theta \int_0^{2\pi} d\phi L_i(\Theta, \Phi, \theta, \phi) t_i$, where p and s indicate the s and p polarization of the incident light and $t_{(s,p)}$ are the Fresnel transmission coefficients. The collection efficiency calculated in this way accounts only for the losses at the interface between the dipole and the substrate. In Fig. 3(b) we show the saturation count rates and the collection efficiency of the Cr emitters. The collection efficiency is calculated using FDTD, assuming an average radius of the NDs of 120 nm (as measured by
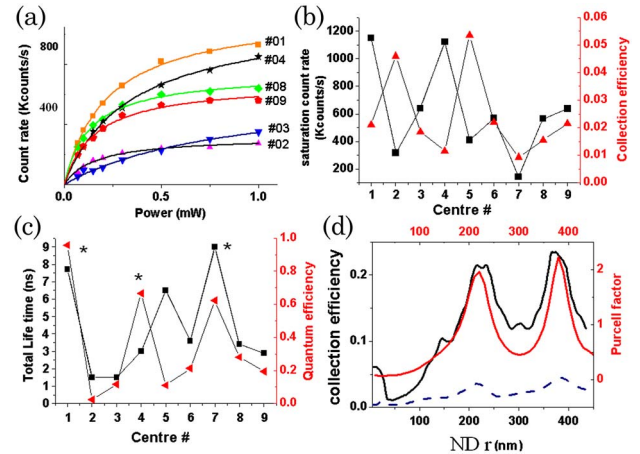
Fig. 3.   (Color online) (a) Saturation curves of the emitters versus optical power, fitted using Origin software yielding a $\chi_\nu^2 = 4 \div 30$ and $r^2 = 0.999$. In some cases the emitters do not reach complete saturation thus reducing the accuracy of the fitting, however, higher power could not be used due to the increased background attributed to high scattering; (b) calculated collection efficiency for the measured dipoles (red triangles on the right axis). The saturation count rates are shown on the left axis (black squares). (c) Total excited state lifetime measurements (left axis, black squares) and quantum efficiency (right axis, red triangles), deduced from the collection efficiency in (b). Stars indicate 2-level system emitters. (d) FDTD calculation of the Purcell factor (right axis) for a Cr center, plotted versus the ND radius (solid red line for a dipole parallel to the substrate plane). On the left axis collection efficiency calculated via FDTD versus the ND radius, black straight curve and dashed blue line for a dipole parallel and orthogonal to the surface, respectively.
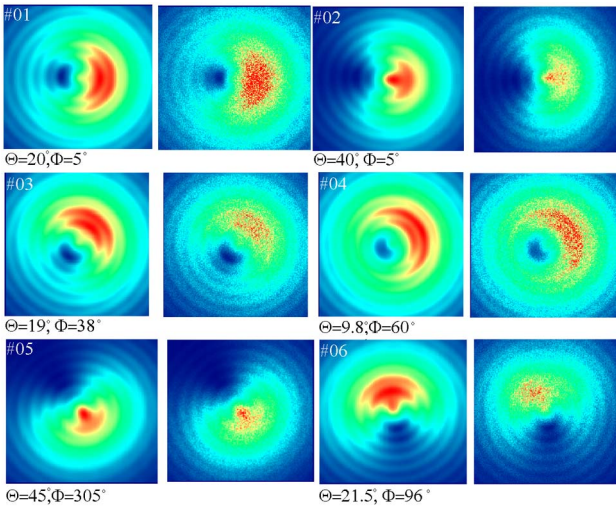
Fig. 2.   (Color online) Defocused dipole imaging of some of the centers studied: on the left the calculated image using FDTD (NA = 0.95 and defocusing of 1.32 μm) and on the right the measured image. Θ and Φ angles are determined. The scale is $4 \times 4 \, \mu$m.

SEM in [5]), integrating over the specific bandwidth of the considered centers and using the measured dipole orientations (Fig. 2). A ND is simulated as a sphere and the dipole is at its center. The calculated collection efficiency by FDTD is validated by the theoretical model for a ND of 10 nm radius. In Fig. 3(c) the total lifetime directly measured is shown and compared to the deduced quantum efficiency from the data in Fig. 3(b). In this case we observe a correlation between emitters with a longer lifetime and highest quantum efficiency, suggesting that shorter lifetimes can be associated to nonradiative decay rates. From the lifetime measurements, it is evident a huge variability, from 1.5 ns to 8 ns and even longer lifetime of 14 ns are measured in similar emitters. This variation occurs for small difference in the spectral emission of the observed Cr centers. The wide variability of lifetime emission of the Cr centers in NDs can be also related to the size of the NDs. We calculate using FDTD the modification of the radiative lifetime due to the ND size for the Cr center. We determine the ratio of the radiative decay rate in NDs with respect to the radiative decay rate in the bulk material ($\propto$ ratio to the local density of states, i.e. Purcell factor). The results are shown in Fig. 3(d): for NDs with radius approaching 180 nm, Mie scattering resonance inside the ND mediates the radiative emission of the dipole, inducing an oscillating Purcell factor larger than 1. As opposite in the case of smaller ND ($r \ll \lambda$) the electrostatic approximation holds and the radiative emission does not depend on the location of the dipole in the sphere and on its orientation. The Purcell factor in the Mie scattering regime depends also on the dipole orientation and the location of the dipole in the diamond. Along this line a direct correlation between lifetime and brightness is not expected in NDs that can hold Mie scattering modes. We also calculate the collection efficiency for different NDs radii. A strong dependence, following the Purcell factor, on the ND size is outlined. The lack of a specific ND's size measurement for the single emitters studied here allow to estimate an average nonradiative decay rate. A direct measurement of the size of the NDs, an experimental validation of size and dipole-distance to the interface effects will be an important addition to determine more accurately the presence of purely nonradiative decay rates.

In summary, we demonstrate a measurement and a methodology to estimate nonradiative decay rates of single defects in NDs. We demonstrate that dipole defocused imaging of single Cr defects in NDs and a more accurate calculation of the collection efficiency dependence on the NDs size are needed in the determination of nonradiative decay rates. Our methods show a quantum efficiency close to 1 in a 2-level system single emitter. We also show that Cr-related centers in NDs with a 3-level system photon statistics present clear nonradiative decay rates. Our modeling and measurements should be considered in the case of designing relevant photonics structures to enhance the collection efficiency of defects in NDs, aiming at highly desirable values of collection efficiency around 90% [10]. Our work will significantly contribute to enhancing present NDs based single photon sources.

References

1. I. Aharonovich, S. Castelletto, D. A. Simpson, C. H. Su, A. G. Greentree, S. Prawer, Rep. Prog. Phys. **74**, 076501 (2011).
2. G. Balasubramanian, I. Y. Chan, R. Kolesov, M. Al-Hmoud, J. Tisler, C. Shin, C. Kim, A. Wojcik, P. R. Hemmer, A. Krueger, T. Hanke, A. Leitenstorfer, R. Bratschitsch, F. Jelezko, and J. Wrachtrup, Nature **455**, 648 (2008)
3. E. Rittweger, K. Y. Han, S. E. Irvine, C. Eggeling, and S. W. Hell, Nat. Photon. **3**, 144 (2009)
4. A. Gruber, A. D. Benstedt, C. Tietz, L. Fleury, J. Wrachtrup, and C. von Borczyskowski, Science **276**, 2012 (1997)
5. I. Aharonovich, S. Castelletto, D. A. Simpson, A. Stacey, J. McCallum, A. D. Greentree, and S. Prawer, Nano Lett. **9**, 3191 (2009)
6. I. Aharonovich, S. Castelletto, Brett C. Johnson, J. C. McCallum, D. A. Simpson, A. D. Greentree, and S. Prawer, Phys. Rev. B **81**, 121201R (2010)
7. S. Castelletto, I. Aharonovich, B. C. Gibson, B. C. Johnson, S. Prawer, Phys. Rev. Lett. **105**, 217403 (2010).
8. B. Butchler, T. Kalkbrenner, C. Hettich, and V. Sandoghdar, Phys. Rev. Lett. **95**, 063003 (2005)
9. X. Brookmann, L. Coolen, M. Dahan and J. P. Hermier, Phys. Rev. Lett. **93**, 107403 (2004)
10. K. G. Lee, X. W. Chen, H. Eghlidi, P. Kukura, R. Lettow, A. Renn, V. Sandoghdar, and S. Götzinger, Nat. Photon. **5**, 166 (2011)